AGU PUBLICATIONS

JGR

Journal of Geophysical Research: Space Physics

RESEARCH ARTICLE
10.1002/2015JA021673

Key Points:
- PC1 yields solar flux-modulated semiannual variation of equatorial magnetic field at all LT
- Semiannual variation disappears in afternoon hours for all solar flux levels with addition of PC2
- Equatorial magnetic field PC3 amplitude has annual variation during extended solar minimum

Correspondence to:
A. Bhattacharyya,
abh@iigs.iigm.res.in

Citation:
Bhattacharyya, A., and K. C. Okpala (2015), Principal components of quiet time temporal variability of equatorial and low-latitude geomagnetic fields, *J. Geophys. Res. Space Physics*, *120*, doi:10.1002/2015JA021673.

Received 11 JUL 2015
Accepted 1 SEP 2015
Accepted article online 5 SEP 2015

Principal components of quiet time temporal variability of equatorial and low-latitude geomagnetic fields

Archana Bhattacharyya[1] and Kingsley C. Okpala[2]

[1]Indian Institute of Geomagnetism, Navi Mumbai, India, [2]Department of Physics and Astronomy, University of Nigeria, Nsukka, Nigeria

Abstract Diurnal variations of the horizontal component of the geomagnetic field ΔH on International Quiet days of 1999–2012, measured hourly at two stations in the same longitude zone in the Northern Hemisphere, near and away from the dip equator, have been subjected to principal component analysis. This technique is also applied to the difference ΔH_{EEJ} of ΔH at these two stations, which is attributed to the equatorial electrojet (EEJ). The first three principal components, PC1–PC3, account for 91–96% of the variances in the data. Maximum contribution to the quiet day variations in ΔH around its peak in the morning hours at both the stations, and in the EEJ, comes from the day-to-day variation of the amplitude of PC1. Patterns of day-to-day variations of PC1 amplitudes for the equatorial station and the EEJ are essentially semiannual modulated by solar EUV flux, superimposed on a longer timescale solar EUV flux-dependent trend. Contributions from PC2 and to a lesser extent from PC3 are seen to be responsible for the absence of semiannual variations in ΔH in the afternoon hours at the equatorial station. Distribution of amplitudes of PC2 and PC3 for ΔH_{EEJ} for weak electrojet days shows seasonal features in accordance with greater occurrence of afternoon (morning) counter electrojet during June (December) solstice. During the extended solar minimum, PC3 amplitudes for ΔH at the equatorial station and for the EEJ display annual variation. Possible sources for these seasonal features in the variations of equatorial ΔH are discussed.

1. Introduction

Identification of the sources that contribute to the quiet time variability in the pattern of regular daily variations of the geomagnetic field measured at locations close to the magnetic equator and at low latitudes continues to be a problem of interest as this is basic to understanding the impact on the equatorial and low-latitude ionosphere of forcing from below. It was established nearly five decades ago from ground geomagnetic observations that a large-scale current system in the low and middle geomagnetic latitude ionosphere, the solar quiet (*Sq*) current system, gives rise to the regular daily variation of the geomagnetic field recorded at low-latitude stations during geomagnetic quiet days [*Matsushita and Maeda*, 1965]. The *Sq* current system is produced by the ionospheric wind dynamo which arises when charged particles in the *E* region of the ionosphere are driven across the Earth's magnetic field by atmospheric winds, setting up currents and electric fields [*Stening*, 1969; *Richmond et al.*, 1976; *Richmond*, 1989]. Over the dip equator, where Earth's magnetic field is horizontal and northward, an eastward electric field gives rise to a vertically downward Hall current which sets up a large vertical electric field due to the limited vertical extent of the electrically conducting *E* region, and this vertical electric field produces a large eastward Hall current, greatly enhancing the net eastward current in a narrow latitudinal belt of approximately $\pm$ 3° about the dip equator. This enhanced current, which flows in the *E* region at altitudes between about 100 and 110 km, is the equatorial electrojet (EEJ), which has been studied over many decades [*Chapman and Raja Rao*, 1965; *Fambitakoye and Mayaud*, 1976; *Forbes*, 1981; *Rastogi*, 1989; *Stening*, 1991; *Onwumechili*, 1997; *Lühr et al.*, 2004; *Alken and Maus*, 2007; *Lühr and Manoj*, 2013]. However, it is still debated whether the EEJ constitutes a separate current system from the *Sq* current system although no separate driving mechanism for the EEJ has been established so far apart from the wind dynamo, which drives the *Sq* current system. Model simulations of the EEJ so far have considered it to be a part of the *Sq* current system [*Doumbia et al.*, 2007; *Fang et al.*, 2008; *Yamazaki et al.*, 2014a, 2014b].

In the wind dynamo region, global-scale motion of the neutral atmosphere is governed by upward propagating solar tides, which are generated in the lower atmosphere by absorption of solar radiation by H_2O in the

troposphere and by O_3 in the stratosphere, and also by nonpropagating diurnal tide driven in situ in the thermosphere above 100 km by solar ultraviolet heating [*Hagan et al*., 2001]. Hence, tides generated in situ in the thermosphere as well as upward propagating tides have been included in modeling the ground magnetic field produced by the EEJ [*Doumbia et al*., 2007; *Yamazaki et al*., 2014a]. Using the National Center for Atmospheric Research (NCAR) Thermosphere-Ionosphere Electrodynamics general circulation model (TIE-GCM) with tidal perturbations at the lower boundary of the model specified by the Thermosphere-Ionosphere-Mesosphere Energetics and Dynamics (TIMED) satellite observations, *Yamazaki et al*. [2014a] suggested that the semiannual variation in the daily range of the horizontal component (H) of the equatorial geomagnetic field, with equinoctial maxima, is mostly due to the upward propagating migrating semidiurnal tide. However, since they used lower boundary tides derived from 60 day averages of temperature and wind data from the TIMED satellite, their model results could not reproduce the significant day-to-day variability seen in the observed data even for quiet days. In a more recent paper, *Yamazaki et al*. [2014b] have attempted to model the day-to-day variations of the EEJ during quiet periods using the NCAR thermosphere-ionosphere-mesosphere electrodynamics general circulation model (TIME-GCM) in which variable forcing of the ionosphere from the lower atmosphere is introduced [*Liu et al*., 2013]. Their model results for Tirunelveli tend to underestimate ΔH during the morning hours and overestimate it during the afternoon hours.

In the present paper, variations ΔH in the horizontal component of the geomagnetic field, recorded on International Quiet (IQ) days of the years 1999–2012, at a station close to the dip equator and another station away from the dip equator and the difference, ΔH_{EEJ}, between the two have been subjected to principal component analysis (PCA). The first three principal components, which account for more than 91% of the variances in the three cases, are used to identify the contributions of these components to the seasonal variation of ΔH at different local times. A feature of the observed semiannual variation in the strength of the EEJ that continues to be an enigma is that it is much more prominent in the morning hours than in the afternoon hours, when it is not visible anymore [*Stening*, 1991; *Rastogi et al*., 1994]. *Yamazaki et al*. [2014a] have suggested that tides generated in the thermosphere acting alongside upward propagating tides may give rise to this situation. Results obtained in the present paper suggest some other possible scenarios. The distinctly different distributions of the amplitudes of the second and third principal components for ΔH_{EEJ} for weak electrojet days during summer and winter solstice months, which are compatible with the known seasonal pattern of occurrence of the morning and afternoon counter electrojet (CEJ) [*Rastogi*, 1974; *Fambitakoye and Mayaud*, 1976: *Mayaud*, 1977; *Vichare and Rajaram*, 2011], are also discussed in the context of these alternate scenarios.

2. Principal Component Analysis of ΔH Variations

Hourly values of the horizontal component H of the geomagnetic field at an equatorial station, Tirunelveli (8.7°N, 77.8°E, geomagnetic latitude ~ 0.2°S), and at a low-latitude station Alibag (18.6°N, 72.9°E, geomagnetic latitude ~ 10°N) away from the dip equator, for five IQ days in each month of the years 1999–2012, where available have been used in this study. During this period, geomagnetic latitude of Tirunelveli changed from 0.41°S to 0.06°N, while for Alibag the corresponding change in geomagnetic latitude was from 9.86°N to 10.30°N. Midnight values of H have been taken as the average of the values for 2330 LT on the previous day and 0030 LT, where LT refers to 75°E local time. Any noncyclic variations in the data have been removed in the manner suggested by *Mann and Schlapp* [1985] to obtain the hourly values of ΔH at Tirunelveli (TIR) and Alibag (ABG) for 794 IQ days, when data from both the locations were available. In the present study, the EEJ is treated as a distinct current system from the *Sq* current system as far as variability of the EEJ currents is considered. The EEJ strength, ΔH_{EEJ}, is simply obtained from $\Delta H_{TIR} - \Delta H_{ABG}$ as has been the practice in many studies [e.g., *Anderson et al*., 2002; *Stolle et al*., 2008]. According to this picture, ΔH_{TIR} has contributions from both the global *Sq* current system and the localized (in latitude) EEJ currents, and the contribution to ΔH_{TIR} from the *Sq* current system is approximated by ΔH_{ABG}. In the past, PCA has been applied to equatorial and low-latitude geomagnetic data for the quiet days in July 1995 to study the CEJ phenomenon [*Gurubaran*, 2002].

In each of the three cases, the 25 hourly values ΔH_{ij} for the ith day (d_i) in the series, and with the integer j varying from 1 to 25, to represent 75°E LT in hours, extending from midnight to midnight, define the pattern

of variation of ΔH for that day. For the jth hour of the ith day, deviation D_{ij}, of ΔH_{ij} from the average value for that hour for all the N (= 794) days under consideration is given by

$$D_{ij} = \Delta H_{ij} - \frac{1}{N}\sum_{k=1}^{N} \Delta H_{kj} \tag{1}$$

This deviation may be expressed in terms of the principal components (PCs), which constitute a set of orthonormal basis functions:

$$D_{ij} = \sum_{k\,=\,1}^{M} S_{ik} P_{kj} \tag{2}$$

Here M represents the maximum number of principal components required to capture the variability of D_{ij} and necessarily satisfies $M \leq 25$; S_{ik} is the factor score or projection of the hourly deviations D_{ij} for the day d_i on to the kth principal component, which is defined by its 25 hourly values P_{kj}. Orthonormality of the PCs implies that

$$\sum_{j\,=\,1}^{25} P_{lj} P_{mj} = \delta_{lm} \tag{3}$$

As D_{ij} is in unit of nanoteslas, S_{ij} is also in unit of nanoteslas. With $\mathbf{D}$ as a 794 $\times$ 25 matrix with elements D_{ij}, a 25 $\times$ 25 covariance matrix $\mathbf{C}$ for the 25 sets of N (= 794) deviations, D_{ij} is obtained as follows:

$$\mathbf{C} = \frac{1}{N-1}\mathbf{D}^{\mathrm{T}}\mathbf{D} \tag{4}$$

where $\mathbf{D}^{\mathrm{T}}$ is the transpose of $\mathbf{D}$ so that $(\mathbf{D}^{\mathrm{T}})_{ji} = \mathbf{D}_{ij}$. Thus, the elements C_{kl} of the covariance matrix are computed from

$$C_{kl} = \frac{1}{N-1}\sum_{i=1}^{N} D_{ki}^{\mathrm{T}} D_{il} = \frac{1}{N-1}\sum_{i=1}^{N} D_{ik} D_{il} \tag{5}$$

The PCs are the eigenvectors of the 25 $\times$ 25 covariance matrix $\mathbf{C}$. The mean value of ΔH for each hour over 794 IQ days that include all seasons yields an average daily pattern independent of seasons. The hourly values of deviations D_{ij} of ΔH_{ij} from this average pattern for each of the 794 IQ days are caused by various factors, some known such as the solar flux and seasons and other factors that are not known. The idea behind application of PCA [e.g., *Jolliffe*, 2002] to the data is to explore the possibility of describing the variability of the daily patterns in terms of fewer parameters than the 25 hourly values such that factors that contribute to the quiet time variability may be investigated more easily and their contributions modeled accordingly. The PCs are identified with basic patterns which account for the largest variability of D_{ij} from 1 day to another. As the PCs are orthonormal, projection of the deviations D_{ij} on to the PCs yields a new set of variables that define the pattern of variation of ΔH for each day. The score factor or projection for the ith day's variations on to the mth principal component is obtained using equations (2) and (3):

$$S_{im} = \sum_{l=1}^{25} D_{il} P_{ml} \tag{6}$$

The covariance matrix for this new set of variables is diagonal. The kth diagonal value in this matrix is the variance associated with the kth PC. The PCs are ranked according to the variance in the data they account for. Thus, the basis function represented by the first PC (PC1) accounts for the largest variance in the data, PC2 the second largest, and so on. In this study computations are carried out by using PCA tools available in MATLAB Statistics toolbox. The first three PCs: PC1–PC3 for ΔH_{TIR}, ΔH_{ABG}, and ΔH_{EEJ} are shown in the three panels in Figure 1a. In each case the score factors or amplitudes for these three components on a given day determine the contributions of the respective PCs to the departure of that particular day's pattern of variation from the mean pattern. Hence, it is not important whether a particular PC in one case is inverted or not, as it has to be multiplied by the corresponding amplitude to determine the contribution of that PC to the variation from the mean pattern [*Stening et al.*, 2005]. In this paper attention is focused on the first three PCs because together they account for around 95%, 91%, and 96% of the variances in the data for ΔH_{TIR}, ΔH_{ABG}, and ΔH_{EEJ}, respectively, as shown in Figure 1b. It may be noted from the patterns of PC1–PC3 for the EEJ that the contribution

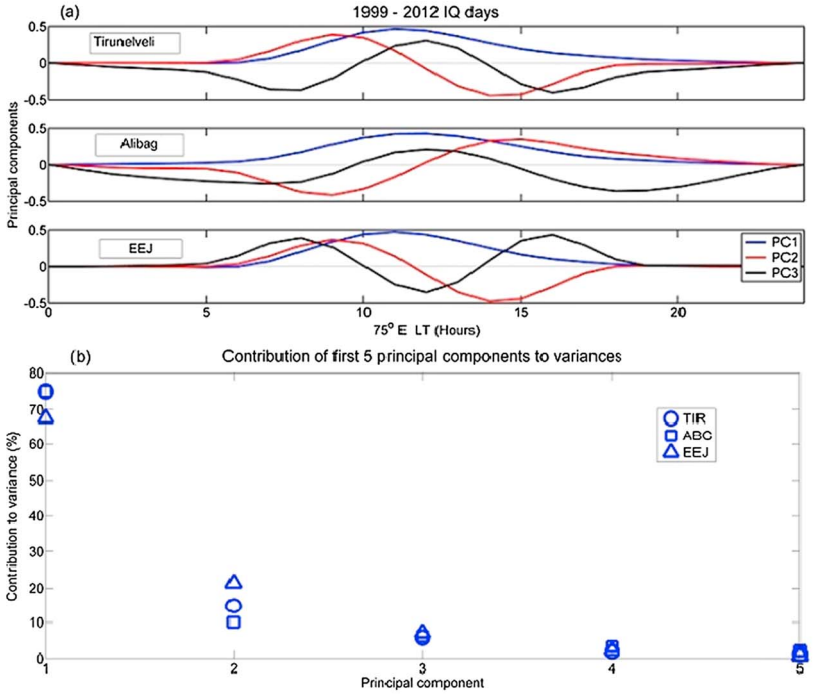

Figure 1. (a) First three principal components computed from ΔH_{TIR}, ΔH_{ABG}, and ΔH_{EEJ} for 794 IQ days during the years 1999–2012; (b) percentage contribution of the first five principal components to the variability of ΔH_{TIR}, ΔH_{ABG}, and ΔH_{EEJ}, respectively.

of PC2 is critical for the occurrence of a morning or afternoon CEJ on a particular day, and the contribution of PC3 also plays a role in determining the local time of occurrence and strength of the CEJ.

3. Contributions of the First Three Principal Components

For the 794 IQ days from the years 1999–2012, used in the present study, the observed daily 10.7 cm solar flux Sf in unit of 10^{-22} W m^{-2} Hz^{-1}, varied between 65.4 and 263.7. In order to identify the influence of solar EUV flux, for which Sf is used as a proxy, and of seasonal variations, on the amplitudes of the first three PCs in each case, Sf, and the daily amplitudes of PC1–PC3 for ΔH_{TIR}, ΔH_{ABG}, and ΔH_{EEJ}, respectively, are plotted as a function of day number starting from 1 January 1999 in Figure 2. For the equatorial station Tirunelveli, amplitude of PC1 clearly shows a semiannual variation with equinoctial maxima, modulated by the solar EUV flux and superimposed on a longer timescale solar EUV flux-dependent trend. PC1 amplitudes for ΔH_{TIR} show significantly larger peaks in the March equinox compared to the September equinox during the years 2000, 2002, and possibly 2008, which may be due to the Mesospheric Quasi-Biennial enhancement of the westward winds observed at an altitude of 96 km over several low-latitude locations including Tirunelveli [*Venkateswara Rao et al.*, 2012]. These authors also reported enhanced westward winds over Tirunelveli in 2006. Based on temperature measurements from the Sounding of the Atmosphere using Broadband Emission Radiometry instrument on the TIMED satellite for the period 2002–2007, *Forbes et al.* [2008] as well as *Mukhtarov et al.* [2009] reported that the amplitudes of DW1 tides at 100 km altitude have equatorial maxima during March–April of years 2002, 2004, and 2006. *Mukhtarov et al.* [2009] also found that the magnitude of the quasi 2 year amplitude peaks diminished over the 6 year period (2002–2007). It is noted that the ground observations of winds have contributions from migrating as well as nonmigrating tides. The PC1 amplitudes for ΔH_{TIR} did not show any enhancement during the March equinox compared to the September equinox of 2006.

As far as the amplitudes of PC1 computed from ΔH_{EEJ} are concerned, they also display a semiannual variation with equinoctial maxima for all the years considered, modulated by the solar EUV flux, although not as clearly as in the case of ΔH_{TIR}. There is a hint of semiannual variations in PC1 amplitudes for Alibag during the high

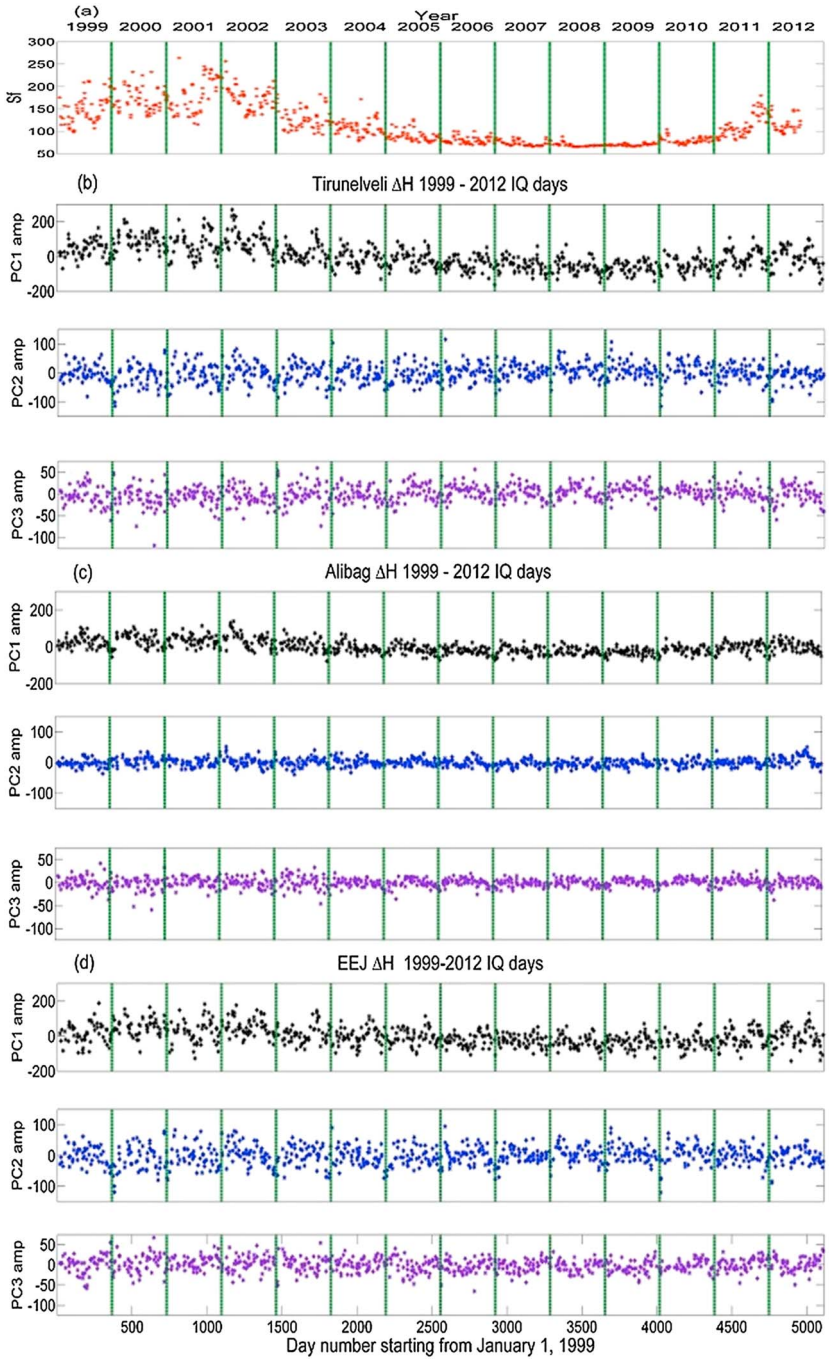

Figure 2. (a) Observed daily 10.7 cm solar flux in units of 10^{-22} W m^{-2} Hz^{-1}, for 794 IQ days from the years 1999–2012; (b–d) daily amplitudes (in nT) of the first three principal components, computed using ΔH_{TIR}, ΔH_{ABG}, and ΔH_{EEJ}, respectively, for the 794 IQ days.

solar flux years of 2000–2002. To a lesser extent, some seasonal variation is also seen in PC2 amplitudes for Tirunelveli and the EEJ during 2000–2002. It is clear that other sources also contribute significantly to these variations. The PC3 amplitudes, however, display an annual variation clearly during low solar flux years, particularly for Tirunelveli and the EEJ. PC3 amplitudes for Tirunelveli and the EEJ are anticorrelated as the respective principal components have opposite patterns, but their contributions to the variability of ΔH_{TIR} and ΔH_{EEJ} would follow the same seasonal pattern. The amplitude of PC3 for ΔH_{EEJ} tends to maximize during the Northern Hemisphere winter solstice and is minimum during the summer solstice. Possible relationships

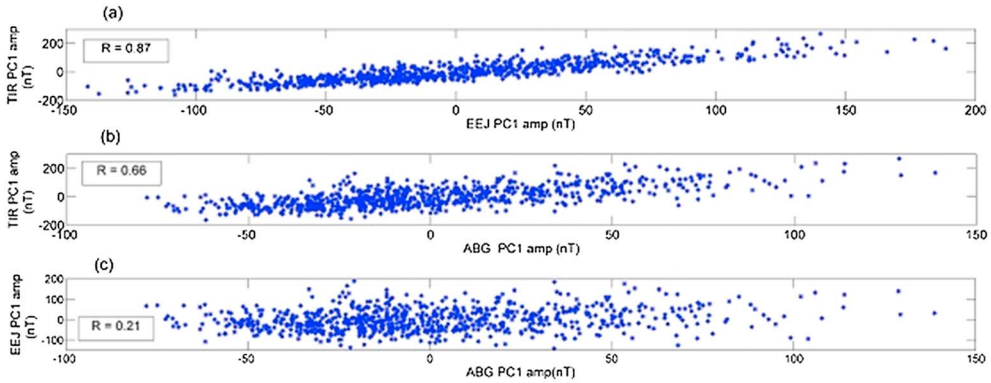

Figure 3. (a) Plot of amplitude of PC1 for ΔH_{TIR} versus amplitude of PC1 for ΔH_{EEJ} for 794 IQ days from the years 1999–2012; (b) same as Figure 3a for ΔH_{TIR} and ΔH_{ABG}; (c) same as Figure 3a for ΔH_{EEJ} and ΔH_{ABG}. The respective correlation coefficients for each case are indicated in the figures.

between the daily amplitudes of PC1, the dominant mode of variation, obtained for ΔH_{TIR}, ΔH_{ABG}, and ΔH_{EEJ} are explored in Figure 3. This figure indicates that the amplitudes of PC1 for ΔH_{TIR} and ΔH_{EEJ} are well correlated ($R = 0.87$) as are the amplitudes of PC1 for ΔH_{TIR} and ΔH_{ABG} ($R = 0.66$) with a significance level < 0.005. However, the amplitudes of PC1 for ΔH_{ABG} and ΔH_{EEJ} show poor correlation ($R = 0.21$). The amplitudes of PC2 for ΔH_{TIR} and ΔH_{EEJ} are well correlated ($R = 0.92$), while the amplitudes of PC3 for ΔH_{TIR} and ΔH_{EEJ} are anticorrelated ($R = -0.86$), the negative sign appearing because PC3 for ΔH_{EEJ} has peaks and troughs that anticorrelate with the corresponding features of PC3 for ΔH_{TIR} (Figure 1a); although these are not shown. Amplitudes of PC2 for ΔH_{TIR} and ΔH_{ABG} show weak anticorrelation ($R = -0.28$); however, the amplitudes of PC3 for ΔH_{TIR} and ΔH_{ABG} show better correlation ($R = 0.55$) with a significance level < 0.005. All other possible combinations of amplitudes of the first three principal components in the three cases show poor correlation or anticorrelation ($|R|^2 \leq 0.1$).

4. Results and Discussion

4.1. Local Time Dependence of Semiannual Variation

The semiannual variation is a well-known feature of the strength of the EEJ as reflected in the peak ΔH at an equatorial station [*Chapman and Raja Rao*, 1965; *Yacob*, 1966; *Rastogi and Iyer*, 1976; *Rastogi et al*., 1994; *Alken and Maus*, 2007], which is captured by the amplitudes of PC1 for ΔH_{TIR} at different levels of solar activity, as can be seen from Figure 2b. From the nature of the first three principal components for ΔH_{TIR} displayed in Figure 1a, it is clear that PC1 contributes the most to day-to-day variations of quiet time ΔH_{TIR} in the morning hours close to 11 LT. Its contribution to the day-to-day variations of ΔH_{TIR} in the afternoon hours is much smaller and may be obliterated by the contributions of PC2 and PC3. This is seen in Figure 4, where the reconstructed ΔH at the equatorial station Tirunelveli for the 794 IQ days under consideration, by adding to the mean pattern (a) only the first component PC1, (b) the first two components PC1 and PC2, and (c) the first three components PC1, PC2, and PC3, is plotted for two different local times, 11 LT and 14 LT. It is clear that while inclusion of PC2 and PC3 amplitudes in the reconstruction does not significantly alter the semiannual pattern of variation seen in ΔH_{TIR} at 11 LT reconstructed with the addition of PC1 amplitude alone, the situation is different at 14 LT. In the afternoon hours the semiannual pattern is considerably weakened by the addition of PC2 amplitudes in the reconstruction. It is mentioned in section 1 that *Yamazaki et al*. [2014a] have carried out simulations of the ground magnetic effects of the equatorial electrojet using the TIE-GCM driven by TIMED satellite data, to demonstrate that the observed semiannual variation in the daily range of ΔH at dip equatorial locations cannot be explained by the thermospherically generated nonpropagating diurnal tide and is mostly due to upward propagating tides. The daily range would be determined by the maximum value of ΔH, which at Tirunelveli is generally attained at around 11 LT. A wind system that contributes to a PC2 pattern of variation in ΔH, as discussed in the next section, is expected to quench the semiannual variation in the afternoon hours as the PC2 amplitudes do not vary in this manner.

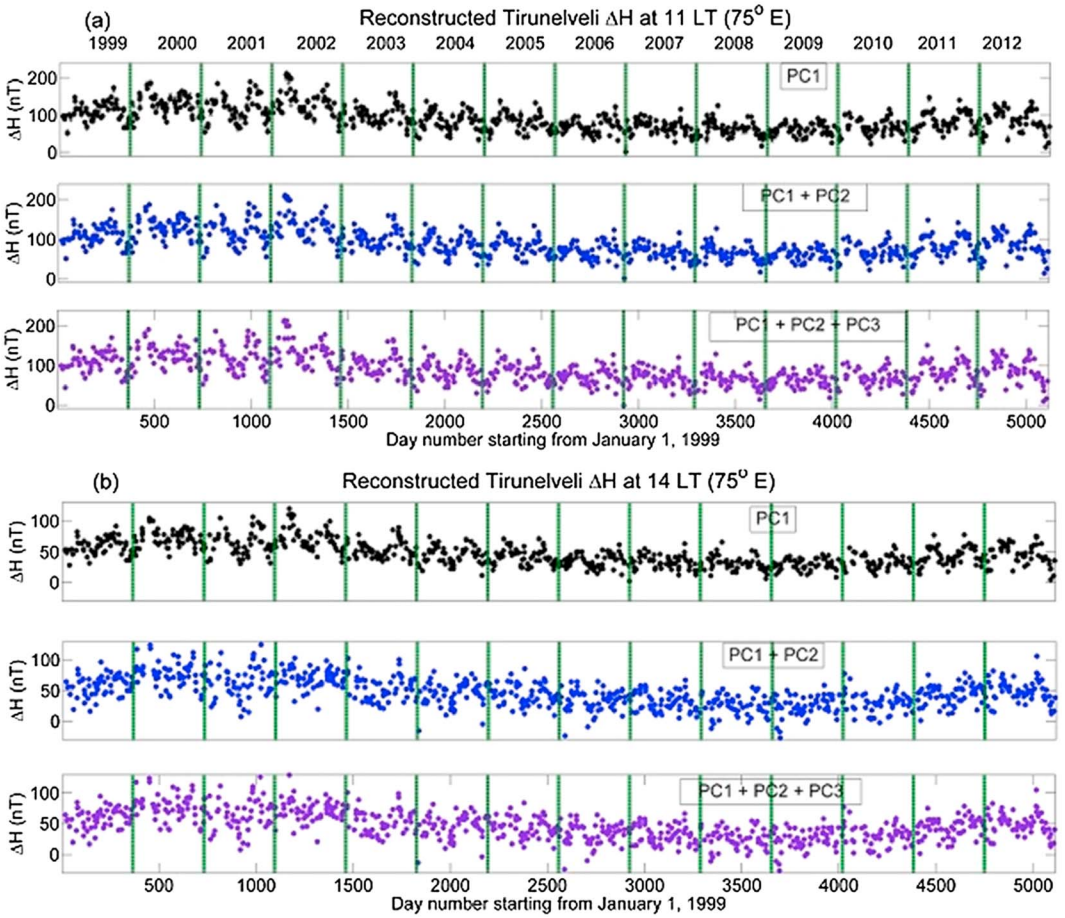

Figure 4. (a) Reconstructed ΔH at 11 LT (75°E) for 794 IQ days during 1999–2012, for the equatorial station, Tirunelveli, using (top) only PC1 amplitudes, (middle) PC1 and PC2 amplitudes, and (bottom) PC1–PC3 amplitudes. (b) Same as Figure 4a at 14 LT (75°E).

4.2. Distribution of PC2 and PC3 Amplitudes on Weak Electrojet Days

TIE-GCM simulations of ΔH at Tirunelveli for the year 2008 using TIMED lower boundary tides [*Yamazaki et al*., 2014a] captured the seasonal variation of ΔH in the prenoon hours but failed to do so for the afternoon hours. The local time pattern of the average difference between observed ΔH at Tirunelveli during May and June 2009 and ΔH simulated using TIME-GCM together with a model that introduced variable lower atmospheric forcing [*Liu et al*., 2013], shown in Figure 3c of *Yamazaki et al*. [2014b], resembles the temporal pattern of PC2 for ΔH_{TIR} or ΔH_{EEJ} obtained in the present study. As discussed in the previous section, PC2 amplitudes play a critical role in determining the day-to-day variation of quiet time ΔH_{TIR} in the afternoon hours around 14–15 LT. At later local times, PC3 amplitudes also make significant contributions. On the basis of known occurrence patterns of morning and afternoon CEJ in different seasons [*Rastogi*, 1974; *Fambitakoye and Mayaud*, 1976: *Mayaud*, 1977; *Vichare and Rajaram*, 2011], it is expected that the distribution of PC2 and PC3 would display some season-specific behavior. This may provide some clues for modeling ΔH at equatorial stations. Both morning and afternoon CEJ occurrences have been found to be anticorrelated with solar activity and the strength of the normal EEJ [*Rastogi*, 1974; *Mayaud*, 1977]. In a global dynamo simulation of ionospheric currents carried out by *Hanuise et al*. [1983], a CEJ event as seen in ground magnetic data was reproduced using a combination of the (2, 2) and (2, 4) solar semidiurnal tidal modes and assuming that the (1, −2) diurnal tide amplitude was negligible. Their results showed the presence of two oppositely directed horizontal current vortices flowing on either side of the noon sector, with anticlockwise flow before noon and clockwise flow in the afternoon. This pattern of currents is compatible with the form of PC2 for ΔH_{TIR} or ΔH_{EEJ}. *Gurubaran* [2002] had applied PCA to geomagnetic data for 19 quiet days of July 1995, from a chain of 11 stations

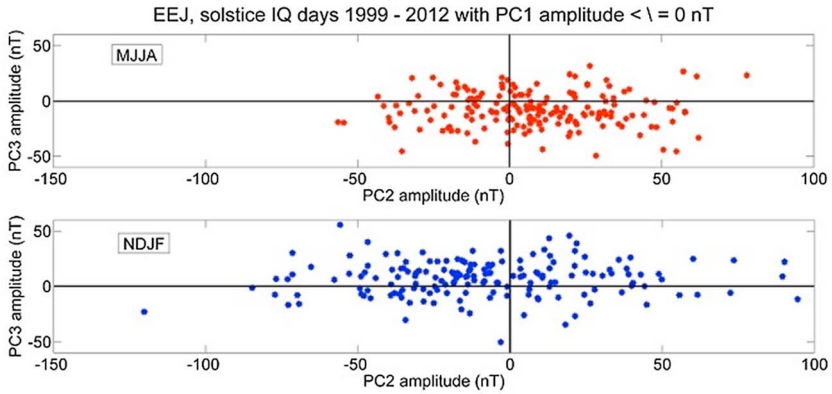

Figure 5. Distribution of PC2 and PC3 amplitudes for the IQ days (top) of the months of May, June, July, and August (MJJA) and (bottom) of the months of November, December, January, and February (NDJF) during 1999–2012, which have lower than average peak strength of ΔH_{EEJ} (PC1 amplitudes ≤ 0).

extending from the dip equator to 59°N dip latitude, and found that on a CEJ day, PC2 to PC5 produced an additional current system with westward flow over the dip equatorial region in the afternoon hours. The focus of this afternoon vortex was located closer to the dip equator than the focus of the *Sq* current system. Also, there was no such clear signature of a current vortex with anticlockwise flow in the morning hours. As may be seen from Figure 1a in the present study, a negative PC3 amplitude for ΔH_{EEJ} on a day with afternoon CEJ would contribute toward weakening of the prenoon vortex obtained by *Hanuise et al.* [1983], while strengthening the postnoon clockwise current flow.

In view of these earlier findings, scatterplots of PC2 and PC3 amplitudes for ΔH_{EEJ}, on IQ days with PC1 amplitudes ≤ 0 such that the peak strengths of ΔH_{EEJ} are lower than average, are presented in Figures 5 (top) and 5 (bottom), for the Northern Hemisphere summer months of May, June, July, and August (MJJA) and winter months of November, December, January, and February (NDJF). Overall, PC2 amplitudes for weak EEJ days tend to be positive during the MJJA months and negative during the NDJF months, while PC3 amplitudes for these days tend to be positive during the NDJF months and negative during the MJJA months. Given the characteristics of PC2 and PC3 for ΔH_{EEJ} displayed in Figure 1a, a positive PC2 amplitude combined with a negative or a small positive PC3 amplitude on a day with weak noontime electrojet would result in an afternoon CEJ. On the other hand, a negative amplitude of PC2 combined with a negative or small positive amplitude of PC3 would result in a morning CEJ. Thus, the distributions shown in Figure 5 are in accordance with the well-known observed patterns of morning and afternoon CEJs. However, the purpose of the present study of the seasonal patterns of distribution of PC2 and PC3 amplitudes is to investigate the possible causes for these distinct patterns. As can be seen from Figure 2d, inclusion of the recent extended solar minimum in this study has revealed a distinct annual pattern of variation of PC3 amplitudes, which may be modeled using specific wind patterns.

The propensity of PC3 amplitudes to be negative during the June solstice months and to be positive during the December solstice months, as noted in an earlier paragraph, could indicate a role of variable meridional winds. Radar observations of mesosphere and lower thermosphere winds over Tirunelveli during 1993–2009 have shown that the monthly mean meridional winds display seasonal characteristics expected from differential heating in the Northern and Southern Hemispheres, the flow being southward during June solstice months and northward during December solstice months [*Sridharan et al.*, 2007]. The Tirunelveli radar data have also indicated that the monthly mean meridional winds at an altitude of 88 km are weak during the years 1999–2003 and become much stronger in the years 2004–2009 [*Venkateswara Rao et al.*, 2012]. Figure 2 shows that the PC3 amplitudes for ΔH_{EEJ} and also ΔH_{TIR} have pronounced annual variations during the years 2005–2009. *Yamazaki et al.* [2014b] showed that the contribution of meridional winds to day-to-day variation of the noontime EEJ is small. In the present study it is seen that large positive or negative amplitudes of PC2 and PC3 have larger contributions to the EEJ in the morning or afternoon hours than at noontime. Hence, it may be important to simulate the effects of meridional winds on the morning and afternoon EEJ.

Apart from the solar semidiurnal tidal modes considered by *Hanuise et al*. [1983] to be the possible source of CEJ currents, *Raghavarao and Anandarao* [1980] used an observed vertical wind profile [*Anandarao et al*., 1978] in a model calculation to show that vertically upward winds in the dip equatorial region can give rise to CEJ in the afternoon. *Anandarao et al*. [1978] attributed the observed vertical wind profile to gravity waves. In an attempt to explain the Equatorial Temperature and Wind Anomaly encountered in DE-2 measurements [*Raghavarao et al*., 1991], *Maruyama et al*. [2003] found that in the vicinity of the equatorial ionization anomaly (EIA) ion drag parallel to the geomagnetic field, produced by the poleward field-aligned ion velocity, accelerates the neutral wind and the resultant divergence at the geomagnetic equator drives an upward neutral wind there, which causes a reduction in the neutral temperature at the geomagnetic equator due to adiabatic cooling. The model calculations of these authors, which are for equinox conditions at 16.8 LT and 72° longitude, show that an upward wind is present down to an altitude of 200 km. However, the electric fields have not been calculated self-consistently in this study. This geomagnetically controlled wind has been found to be suppressed at 10°–30° geomagnetic latitudes [*Miyoshi et al*., 2011]. In the present context, it may also be mentioned that a highly localized lowering of daytime mesopause temperature over the dip equator during some CEJ events has been reported by *Vineeth et al*. [2007]. If a geomagnetically controlled vertically upward neutral wind were to extend to lower altitudes over the dip equator, it could produce a CEJ as demonstrated by *Raghavarao and Anandarao* [1980] and at the same time the occurrence of CEJ at equatorial latitudes would not be accompanied by any correlated changes in $Sq(H)$ away from the dip equator, as has been suggested by several earlier studies [e.g., *Rastogi*, 1992; *Yamazaki et al*., 2009] and by the absence of correlation between the PC1 amplitudes for ΔH_{EEJ} and ΔH_{ABG} evident in Figure 3. This hypothesis seems attractive also because a large positive amplitude of PC2 contributes to a stronger EEJ near its peak around 11 LT and hence a stronger EIA, which would result in a larger upward vertical drift over the geomagnetic equator in the afternoon, while the reverse would happen for a large negative amplitude of PC2. Simulations are required to study the effect of seasonal changes in the offset between the subsolar point and the dip equator, as an explanation is also required for NDJF months having a larger percentage of days with PC2 amplitudes ≤ 0, compared to MJJA months. In addition to an equatorial eastward electric field, meridional winds also play a role in the development of the EIA. Hence, if the developing EIA provides a feedback to the EEJ, meridional winds may contribute to the CEJ. In this scenario, a meridional wind-dependent PC3 amplitude could contribute to the CEJ phenomenon.

5. Summary and Conclusions

Hourly variations, ΔH, in the horizontal component H of the geomagnetic field, on IQ days during the years 1999–2012, at the dip equatorial station Tirunelveli and at Alibag, a station away from the dip equator in the Indian region, have been subjected to principal component analysis. PCA is also applied to the difference ΔH_{EEJ} of ΔH at these two stations, to investigate the possible sources of their variability. Contributions of only the first three principal components: PC1–PC3, to the variability in each case have been considered here because together they account for around 95%, 91%, and 96% of the variances in the data for ΔH_{TIR}, ΔH_{ABG}, and ΔH_{EEJ}, respectively. Results obtained from this analysis are as follows:

1. PC1 amplitudes for ΔH_{TIR} and ΔH_{EEJ} show clear semiannual variations with equinoctial maxima superimposed on a solar EUV flux-dependent longer term trend over the whole period under consideration. Amplitude of the semiannual variation is modulated by the solar EUV flux. PC1 amplitudes for ΔH_{TIR} have significantly larger peaks during the March equinox compared to the September equinox during 2000, 2002, and possibly 2008, which may be due to the Mesospheric Quasi-Biennial enhancement of westward winds as observed over Tirunelveli in March 2000, 2002, and 2008 [*Venkateswara Rao et al*., 2012].
2. ΔH at Tirunelveli on IQ days of the years 1999–2012, reconstructed using only PC1 amplitudes, shows semiannual variations during both morning and afternoon hours. With the addition of PC2 amplitudes in the reconstruction, ΔH at 11 LT (75°E) continue to display semiannual variations, which practically disappear at 14 LT (75°E). Thus, PC2 is the main contributor to the weakening of the semiannual variation at Tirunelveli in the afternoon hours.
3. During the years of low solar activity, in particular, the years 2006–2009, PC3 amplitudes for ΔH_{TIR} and ΔH_{EEJ} exhibit an annual pattern of variation, while no clear seasonal pattern emerges for the PC2 amplitudes.

4. For weak EEJ days with PC1 amplitudes ≤ 0, distribution of amplitudes of PC2 and PC3 for ΔH_{EEJ} shows distinct features for the June and December solstices. During MJJA months, out of the 180 weak EEJ IQ days, only 13% have negative amplitudes for PC2 and positive amplitudes for PC3, while nearly 47% have positive amplitude for PC2 and negative amplitude for PC3. The distribution of PC2 and PC3 amplitudes during NDJF months is just the opposite: out of 165 weak EEJ IQ days, only 11% have positive amplitude for PC2 and negative amplitude for PC3, while 42% have negative amplitude for PC2 and positive amplitude for PC3. While these distributions are in accordance with the known pattern of occurrence of morning and afternoon CEJs, they offer a few possibilities for the wind systems that contribute to the phenomenon, as discussed in the previous section. However, some of the possible physical processes that contribute to the various principal components are, at present, speculations as a full analysis of these ideas is not given in this paper.

Acknowledgments

The geomagnetic field data used in this study are available at the World Data Centre for Geomagnetism, Mumbai, and the adjusted daily 10.7 cm solar flux data are available at the National Geophysical Data Center, NOAA, Boulder, USA. A.B. acknowledges the support received from SERB, Department of Science and Technology, Government of India, in the form of a J.C. Bose National Fellowship. K.C.O. was supported by a C.V. Raman International Fellowship for African Researchers from Department of Science and Technology, Government of India.

Alan Rodger thanks two reviewers for their assistance in evaluating this paper.

References

Alken, P., and S. Maus (2007), Spatio-temporal characterization of the equatorial electrojet from CHAMP, Ørsted, and SAC-C satellite magnetic measurements, *J. Geophys. Res.*, *112*, A09305, doi:10.1029/2007JA012524.

Anandarao, B. G., R. Raghavarao, J. N. Desai, and G. Haerendel (1978), Vertical winds and turbulence over Thumba, *J. Atmos. Terr. Phys.*, *40*, 157–163.

Anderson, D., A. Anghel, K. Yumoto, M. Ishitsuka, and E. Kudeki (2002), Estimating daytime vertical $E \times B$ drift velocities in the equatorial *F* region using ground-based magnetometer observations, *Geophys. Res. Lett.*, *29*(12), 1596, doi:10.1029/2001GL014562.

Chapman, S., and K. S. Raja Rao (1965), The *H* and *Z* variations along and near the equatorial electrojet in India, Africa, and the Pacific, *J. Atmos. Terr. Phys.*, *27*, 559–581.

Doumbia, V. A., A. Maute, and A. D. Richmond (2007), Simulation of equatorial electrojet magnetic effects with the thermosphere-ionosphere-electrodynamics general circulation model, *J. Geophys. Res.*, *112*, A09309, doi:10.1029/2007JA012308.

Fambitakoye, O., and P. N. Mayaud (1976), Equatorial electrojet and regular daily variation S_R—I. A determination of the equatorial electrojet parameters, *J. Atmos. Terr. Phys.*, *38*, 1–17.

Fang, T. W., A. D. Richmond, J. Y. Liu, A. Maute, C. H. Lin, C. H. Chen, and B. Harper (2008), Model simulation of the equatorial electrojet in the Peruvian and Phillipine sectors, *J. Atmos. Sol. Terr. Phys.*, *70*, 2203–2211.

Forbes, J. M. (1981), The equatorial electrojet, *Rev. Geophys.*, *19*(3), 469–504, doi:10.1029/RG019i003p00469.

Forbes, J. M., X. Zhang, S. Palo, J. Russell, C. J. Mertens, and M. Mlynczak (2008), Tidal variability in the ionospheric dynamo region, *J. Geophys. Res.*, *113*, A02310, doi:10.1029/2007JA012737.

Gurubaran, S. (2002), The equatorial counter electrojet: Part of a worldwide current system?, *Geophys. Res. Lett.*, *29*(9), doi:10.1029/2001GL014519.

Hagan, M. E., R. G. Roble, and J. Hackney (2001), Migrating thermospheric tides, *J. Geophys. Res.*, *106*, 12,739–12,752, doi:10.1029/2000JA000344.

Hanuise, C., C. Mazaudier, P. Vila, M. Blanc, and M. Crochet (1983), Global dynamo simulation of ionospheric currents and their connection with the equatorial electrojet and counter electrojet: A case study, *J. Geophys. Res.*, *88*, 253–270, doi:10.1029/JA088iA01p00253.

Jolliffe, I. T. (2002), *Principal Component Analysis*, Springer, New York.

Liu, H.-L., V. A. Yudin, and R. G. Roble (2013), Day-to-day ionospheric variability due to lower atmosphere perturbations, *Geophys. Res. Lett.*, *40*, 665–670, doi:10.1002/grl50125.

Lühr, H., and C. Manoj (2013), The complete spectrum of the equatorial electrojet related to solar tides: CHAMP observations, *Ann. Geophys.*, *31*, 1315–1331, doi:10.5194/angeo-31-1315-2013.

Lühr, H., S. Maus, and M. Rother (2004), Noon-time equatorial electrojet: Its spatial features as determined by the CHAMP satellite, *J. Geophys. Res.*, *109*, A01306, doi:10.1029/2002JA009656.

Mann, R. J., and D. M. Schlapp (1985), The effect of disturbance on the day-to-day variability of *Sq*, *Geophys. J. R. Astron. Soc.*, *80*, 535–540.

Maruyama, N., S. Watanabe, and T. J. Fuller-Rowell (2003), Dynamic and energetic coupling in the equatorial ionosphere and thermosphere, *J. Geophys. Res.*, *108*(A11), 1396, doi:10.1029/2002JA009599.

Matsushita, S., and H. Maeda (1965), On the geomagnetic solar quiet daily variation field during the IGY, *J. Geophys. Res.*, *70*(11), 2535–2558, doi:10.1029/JZ070i011p02535.

Mayaud, P. N. (1977), The equatorial counter-electrojet: A review of its geomagnetic aspects, *J. Atmos. Terr. Phys.*, *39*, 1055–1070, doi:10.1016/0021-9169(77)90014-9.

Miyoshi, Y., H. Fujiwara, H. Jin, H. Shinagawa, H. Liu, and K. Terada (2011), Model study on the formation of the equatorial mass density anomaly in the thermosphere, *J. Geophys. Res.*, *116*, A05322, doi:10.1029/2010JA016315.

Mukhtarov, P., D. Pancheva, and B. Andonov (2009), Global structure and seasonal and interannual variability of the migrating diurnal tide seen in the SABER/TIMED temperatures between 20 and 120 km, *J. Geophys. Res.*, *114*, A02309, doi:10.1029/2008JA013759.

Onwumechili, C. A. (1997), *The Equatorial Electrojet*, Gordon and Breach, Newark, N. J.

Raghavarao, R., and B. G. Anandarao (1980), Vertical winds as a plausible cause for equatorial counter electrojet, *Geophys. Res. Lett.*, *7*, 357–360, doi:10.1029/GL007i005p00357.

Raghavarao, R., L. E. Wharton, N. W. Spencer, H. G. Mayr, and L. H. Brace (1991), An equatorial temperature and wind anomaly (ETWA), *Geophys. Res. Lett.*, *18*(7), 1193–1196, doi:10.1029/91GL01561.

Rastogi, R. G. (1974), Westward equatorial electrojet during daytime hours, *J. Geophys. Res.*, *79*(10), 1503–1512, doi:10.1029/JA079i010p01503.

Rastogi, R. G. (1989), The equatorial electrojet, in *Geomagnetism*, vol. 3, edited by J. Jacobs, pp. 461–525, Academic Press, San Diego, Calif.

Rastogi, R. G. (1992), Critical problems of equatorial electrojet, *Adv. Space Res.*, *12*, 13–21.

Rastogi, R. G., and K. N. Iyer (1976), Quiet day variation of geomagnetic *H*-field at low latitudes, *J. Geomagn. Geoelectr.*, *28*, 461–479.

Rastogi, R. G., S. Alex, and A. Patil (1994), Seasonal variations of geomagnetic *D*, *H*, and *Z* fields at low latitudes, *J. Geomagn. Geoelectr.*, *46*, 115–126.

Richmond, A. D. (1989), Modeling the ionosphere wind dynamo: A review, *Pure Appl. Geophys.*, *47*, 413–435.

Richmond, A. D., S. Matsushita, and J. D. Tarpley (1976), On the production mechanism of electric currents and fields in the ionosphere, *J. Geophys. Res.*, *81*(4), 547–555, doi:10.1029/JA081i004p00547.

Sridharan, S., T. Tsuda, and S. Gurubaran (2007), Radar observations of long-term variability of mesosphere and lower thermosphere winds over Tirunelveli (8.7°N, 77.8°E), *J. Geophys. Res.*, *112*, D23105, doi:10.1029/2007JD008669.

Stening, R. J. (1969), An assessment of the contributions of various tidal winds to the *Sq* current system, *Planet. Space Sci.*, *17*, 889–908.

Stening, R. J. (1991), Variability of the equatorial electrojet: Its relations to the *Sq* current system and semidiurnal tides, *Geophys. Res. Lett.*, *18*(11), 1979–1982, doi:10.1029/91GL02413.

Stening, R., T. Reztsova, D. Ivers, J. Turner, and D. Winch (2005), A critique of methods of determining the position of the focus of the *Sq* current system, *J. Geophys. Res.*, *110*, A04305, doi:10.1029/2004JA010784.

Stolle, C., C. Manoj, H. Lühr, S. Maus, and P. Alken (2008), Estimating the daytime equatorial ionization anomaly strength from electric field proxies, *J. Geophys. Res.*, *113*, A09310, doi:10.1029/2007JA012781.

Venkateswara Rao, N., T. Tsuda, D. M. Riggin, S. Gurubaran, I. M. Reid, and R. A. Vincent (2012), Long term variability of mean winds in the mesosphere and lower thermosphere at low latitudes, *J. Geophys. Res.*, *117*, A10312, doi:10.1029/2012JA017850.

Vichare, G., and R. Rajaram (2011), Global features of quiet time counterelectrojet observed by Ørsted, *J. Geophys. Res.*, *116*, A04306, doi:10.1029/2009JA015244.

Vineeth, C., T. K. Pant, C. V. Devasia, and R. Sridharan (2007), Highly localized cooling in daytime mesopause temperature over the dip equator during counter electrojet events: First results, *Geophys. Res. Lett.*, *34*, L14101, doi:10.1029/2007GL030298.

Yacob, A. (1966), Seasonal parameters of the equatorial electrojet at different longitude zones, *J. Atmos. Terr. Phys.*, *28*, 581–597.

Yamazaki, Y., K. Yumoto, A. Yoshikawa, S. Watari, and H. Utada (2009), Characteristics of counter-*Sq* (SFE*) at the dip equator CPMN stations, *J. Geophys. Res.*, *114*, A05306, doi:10.1029/2009JA014124.

Yamazaki, Y., A. D. Richmond, A. Maute, Q. Wu, D. A. Ortland, A. Yoshikawa, I. A. Adimula, B. Rabiu, M. Kunitake, and T. Tsugawa (2014a), Ground magnetic effects of the equatorial electrojet simulated by the TIE-GCM driven by TIMED satellite data, *J. Geophys. Res. Space Physics*, *119*, 3150–3161, doi:10.1029/2013JA019487.

Yamazaki, Y., A. D. Richmond, A. Maute, H.-L. Liu, N. Pedatella, and F. Sassi (2014b), On the day-to-day variation of the equatorial electrojet during quiet periods, *J. Geophys. Res. Space Physics*, *119*, 6966–6980, doi:10.1002/2014JA020243.